On the Single-Target Accuracy of OFDM Radar Algorithms

Martin Braun*, Thomas Schu*, Christian Sturm‡ and Friedrich K. Jondral*
*Communications Engineering Lab, Karlsruhe Institute of Technology (KIT), Germany
‡Institut für Hochfrequenztechnik und Elektronik, Karlsruhe Institute of Technology (KIT), Germany
{martin.braun, christian.sturm, friedrich.jondral}@kit.edu

***Abstract*—Two OFDM radar algorithms (the Maximum Likelihood and a MUSIC-based algorithm) are introduced and their fundamental limits concerning accuracy are explained. To simplify the analysis, we research the special case of only one target in the radar's detection range, which facilitates the individual effects on the estimation quality. Through simulations, we can show that OFDM radar works well for this case.**

I. Introduction

OFDM signals have become an interesting choice for radar. They allow for separate estimation of target distance and Doppler shift by means of spectral estimation algorithms and can be used to transmit information at the same time. This makes OFDM radar useful for mobile networks, e.g. in car-to-car communication networks, where the additional feature of a radar system has a huge benefit, and does not even require additional spectrum usage or radio hardware.

In this paper, we talk about the fundamental limits of OFDM radar algorithms for the special case when there is only one target within detection range. This simplification reduces applicability in real-world scenarios, but provides a good starting point for more general research and also gives some first insights into how well an OFDM radar works. We will introduce the basics of OFDM radar in the following Section. Section III will explain two OFDM radar algorithms. Next, some limits for OFDM radar will be given in Section IV, empirical results are then shown in Section V. Section VI concludes.

II. OFDM Radar Basics

This section outlines the basics of the OFDM radar system. For a more detailed introduction, we refer to [1]–[3].

The proposed radar system uses OFDM signals to estimate distance and relative speed of targets. For every measurement, an OFDM frame is transmitted, consisting of N sub-carriers and M OFDM symbols. The l-th OFDM symbol contains N modulation symbols $c_{k,l} \in \mathcal{A}$, where $\mathcal{A} \subset \mathbb{C}$ is a modulation alphabet (e.g. BPSK). The relevant parameters are:

- Δf: the sub-carrier distance. The frequency of the k-th sub-carrier is represented by $f_k = f_0 + k\Delta f$.
- T_G: the length of the guard interval.
- $T_O = 1/\Delta f + T_G$: the total duration of one OFDM symbol.

Transmitted OFDM frames are represented as matrices

$$\mathbf{F}_{\text{Tx}} = \begin{pmatrix} c_{0,0} & \cdots & c_{0,M-1} \\ c_{1,0} & \cdots & c_{1,M-1} \\ \vdots & \ddots & \vdots \\ c_{N-1,0} & \cdots & c_{N-1,M-1} \end{pmatrix} \in \mathbb{C}^{N\times M}. \quad (1)$$

Every row of the matrix corresponds to the data on one sub-carrier, whereas every column corresponds to the data on one OFDM symbol. The data encoded on the individual symbols $c_{k,l}$ can be received by other participants, thus enabling dual use of the signal as a communication link.

Synchronously to transmission, a receiver is active which detects the backscattered signals reflected by other objects. Their distance and the relative speed cause a round trip propagation delay τ and a Doppler shift f_D. The received signal in case of H separate targets can thus be written as

$$(\mathbf{F}_{\text{Rx}})_{k,l} = c_{k,l}\sum_{h=0}^{H-1} b_h e^{j2\pi l T_O f_{D,h}} e^{-j2\pi k\tau_h \Delta f} e^{j\varphi_h} + (\mathbf{W})_{k,l}. \quad (2)$$

$\mathbf{W}$ is the matrix representation of additive white Gaussian noise (AWGN); its entries are i.i.d. random variables from a circular, complex, zero-mean normal distribution with variance σ^2. b_h is the attenuation of the h-th signal. All phase shifts which are constant for the entire frame are summarized into the phase terms φ_h. This includes any kind of phase rotation on the channel and is thus unknown at the receiver.

Before further processing, the transmitted information is removed from $\mathbf{F}_{\text{Rx}}$ by element-wise division with $\mathbf{F}_{\text{Tx}}$. This results in a radar reception matrix

$$\begin{aligned}(\mathbf{F})_{k,l} &= \frac{(\mathbf{F}_{\text{Rx}})_{k,l}}{(\mathbf{F}_{\text{Tx}})_{k,l}} \\ &= \sum_{h=0}^{H-1} b_h e^{j(2\pi(lT_O f_{D,h} - k\tau_h\Delta f)) + \varphi_h} + (\mathbf{W}')_{k,l}.\end{aligned} \quad (3)$$

As explained in [3], the statistics of the noise are not affected by the division; $\mathbf{W}'$ is thus a noise matrix with the same statistical properties as $\mathbf{W}$. This becomes obvious for constant-modulus modulations such as BPSK, where $|c_{k,l}| = 1$ is always true.

The estimation of τ and f_D is thus equivalent to the detection of the fundamental frequency of discretely sampled complex sinusoids in WGN. Since time-discrete signals are periodically repeated in the frequency domain, the parameters can only be unambiguously estimated if $T_O f_{D,h} < 1$ and $\tau_h \Delta f < 1$ are true. When applying this to the relation between delay and distance, an unambiguous range for distance can be given by [1]

$$d_{\text{max}} = \frac{c_0 \tau_{\text{max}}}{2} = \frac{c_0}{2\Delta f}. \tag{4}$$

Analogously, the maximum unambiguous range for relative speed is given by [2]

$$v_{\text{max}} = \frac{f_{D,\text{max}} c_0}{2 f_c} = \frac{c_0}{2 f_c \cdot T_O}. \tag{5}$$

c_0 is the speed of light, f_c the signal's centre frequency. Unlike the distance, negative relative velocities are equally likely as positive ones. The unambiguous velocity range is thus bounded by $|v| < v_{\text{max}}/2$.

In order to transform the radar problem into a spectral estimation problem in this manner, several assumptions are made:

1) The receive and transmit front-ends are ideal in the sense that they introduce no non-linear distortions apart from AWGN. This includes a dynamic range large enough even if there is direct coupling between transmit and receive antennas.
2) T_G is greater than the round-trip propagation time of the backscattered signal for the furthermost target.
3) Δf is at least one order of magnitude larger than the Doppler shift caused by the object with the highest relative velocity.
4) The signal's centre frequency is several orders of magnitude larger than its total bandwidth, so the Doppler shift is assumed constant over the entire bandwidth.
5) The target speed is small enough to allow for the assumption that its position is constant during one measurement.

While assumption 1) is of course an idealisation of what exists in reality, assumptions 2) through 4) can be fulfilled by choosing appropriate OFDM parameters, which we discuss in [4]. They ensure the received signal is not de-orthogonalized with respect to the transmit signal. The final assumption is an approximation which will decrease ranging accuracy at high relative velocities; however, in combination with the other assumptions it ensures orthogonality of the estimation problems for range and Doppler and thus simplifies the estimators.

A. Signal-to-noise Ratio

The estimation quality is of course mainly determined by the signal-to-noise ratio (SNR). In the case of one target, we may normalise (3) such that $b_0 = 1$, which yields unit power for the sinusoid and therefore

$$\text{SNR}_{\text{dB}} = -10 \log_{10} \sigma^2. \tag{6}$$

Its value is influenced by a large number of physical parameters, a complete list of which is shown in Table I. These include the radio system setup as well as the distance and radar cross section (RCS[1]) of the target.

TABLE I
RELEVANT PARAMETERS FOR SNR

P_{Tx}	Transmit power
G	Total transmit and receive antenna gain
f_c	Centre frequency
B	Signal bandwidth
$k_B T$	Boltzmann's constant times receiver noise temperature
NF	Total receiver chain noise figure (including digital acquisition)
d	Target distance
σ_{RCS}	Target radar cross section

While the radio system does not change during operation, d and σ_{RCS} depend on the target. By using the point-scatter approximation [6, Ch. 2], we know the received power is determined by

$$P_{\text{Rx}} = \frac{P_{\text{Tx}} G c^2 \sigma_{\text{RCS}}}{(4\pi)^3 f_c^2 r^4}. \tag{7}$$

The receiver induces noise with a total noise power density of $N_0 = k_B T \cdot \text{NF}$. Total SNR is thus

$$\text{SNR} = \frac{P_{\text{Rx}}}{N_0 B} = \frac{P_{\text{Tx}} G c_0^2}{(4\pi)^3 f_c^2 N_0 B} \cdot \frac{\sigma_{\text{RCS}}}{r^4}. \tag{8}$$

It must be pointed out that the signal configuration itself is part of the SNR equation by the relation $B = N\Delta f$. This has effects on the estimator's variance (see Section IV-B).

III. OFDM RADAR ALGORITHMS

A. Maximum Likelihood Estimation

This algorithm is derived in greater detail in our previous work [3]. It is based on the fact that the Maximum Likelihood Estimator (MLE) of a sinusoid's frequency is the maximum value of its periodogram (cf. [7], [8] among others). The estimation algorithm for relative speed and range of the targets is as follows:

1) Run the FFT of length M_{FFT} on every row of $\mathbf{F}$.
2) On the resulting matrix, calculate the IFFT of length N_{FFT} on every column.
3) Calculate the modulus-square of every element of the resulting matrix. The result is the two-dimensional periodogram

$$(\mathbf{C})_{m,n} = \left|\text{IFFT}(n)\left\{\text{FFT}(m)\{\mathbf{F}_{k,l}\}\right\}\right|^2. \tag{9}$$

4) Every reflecting object corresponds to a peak in $\mathbf{C}$. A peak at index values $(\hat{m}, \hat{n})$ corresponds to an object with estimated distance and relative velocity [3]

$$\hat{d} = \frac{\hat{n} c_0}{2 N_{\text{FFT}} \Delta f}, \text{ and } \hat{v} = \frac{\hat{m} c_0}{2 f_c M_{\text{FFT}} T_O}. \tag{10}$$

The indices m for the Doppler shift go from $-M_{\text{FFT}}/2$ to $M_{\text{FFT}}/2 - 1$ as the relative velocity can both be positive or negative, whereas the indices n are counted from 0 up to $N_{\text{FFT}} - 1$. The computational complexity can further be reduced

[1]We use the same RCS value for both frequencies for better comparability; the chosen value is a result of measurements [5]

by defining maximum index values $m_{\max}$ and $n_{\max}$, beyond which no values are calculated. These maximum values can be chosen e.g. to match the assumptions 2) and 3). The FFT and IFFT lengths M_{FFT} and N_{FFT} can be any integer value larger than or equal to M and N, respectively. Choosing a larger value results in zero-padding and therefore can increase the accuracy of the estimate (see Section IV-C).

It is worth pointing out that the estimation of speed and distance are orthogonal problems since the values for τ and f_D do not affect each other in $\mathbf{F}$.

B. MUSIC-Based Estimation

An alternative method to estimate frequencies is the MUSIC algorithm, which is explained in great detail in a multitude of publications (e.g. [8], [9]). For the sake of brevity, only the most important steps are repeated here. Assume $\mathbf{r}_i \in \mathbb{C}^{1\times K}$, $i = 1 \ldots L$, to be independent vector representations of signal containing P complex sinusoids, each with different frequency Ω_i, and AWGN. A maximum likelihood estimate of the signal's autocorrelation matrix is [8]

$$\hat{\mathbf{R}}_{xx} = \frac{1}{L}\sum_{i=0}^{L-1} \mathbf{x}_i^H \mathbf{x}_i \in \mathbb{C}^{K\times K}. \quad (11)$$

MUSIC estimates frequencies by calculating the eigenvalue decomposition of the autocorrelation matrix estimate, $\hat{\mathbf{R}}_{xx} = \mathbf{V}\mathbf{\Lambda}\mathbf{V}^{-1}$. The eigenvectors, which form the columns of the matrix $\mathbf{V}$, can be divided into a signal subspace and a noise subspace by assigning the eigenvectors corresponding to the P largest eigenvalues to the former subspace, and the other $K-P$ vectors to the latter, which shall be denoted $\mathbf{V}_{\text{noise}} \in \mathbb{C}^{K\times(K-P)}$. Due to the nature of the noise space, any sinusoid vector $\mathbf{s}(e^{j\Omega}) = (1, e^{j\Omega}, e^{j2\Omega}, \ldots, e^{j(K-1)\Omega)})^T$ with frequency $\Omega = \Omega_i$ must lie in the null space of $\mathbf{V}_{\text{noise}}$. One way to obtain estimates of the Ω_i is thus to substitute $z = e^{j\Omega}$ and solve for the roots[2] of

$$\mathbf{s}^H(z)\mathbf{V}_{\text{noise}}\mathbf{V}_{\text{noise}}^H\mathbf{s}(z) = 0. \quad (12)$$

In the case of OFDM radar, $\mathbf{F}$ contains independent realisations of the relevant sinusoids on the columns caused by the round trip delay. Analogously, the rows contain realisations of sinusoids caused by the Doppler shifts. The estimation of the range d and the relative velocity v therefore requires two autocorrelation matrices, denoted $\mathbf{R}_d$ and $\mathbf{R}_v$, respectively. From (11), we can see that these matrices can be estimated by

$$\hat{\mathbf{R}}_d = \frac{1}{M}\mathbf{F}\mathbf{F}^H \text{ and } \hat{\mathbf{R}}_v = \frac{1}{N}\mathbf{F}^H\mathbf{F}. \quad (13)$$

The algorithm for estimating a single target with Root-MUSIC-based OFDM radar is thus

1) Calculate $\hat{\mathbf{R}}_d$ and $\hat{\mathbf{R}}_v$ according to (13).
2) Using the matrix $\hat{\mathbf{R}}_d$, calculate the noise subspace and, accordingly, the root $\hat{z}_{d,1}$, of (12) closest to the unit circle. Analogously, calculate the root $\hat{z}_{v,1}$ using $\hat{\mathbf{R}}_d$.
3) Calculate the frequency estimates $\hat{\Omega}_{d,k} = \arg\{\hat{z}_{d,k}\}$ and $\hat{\Omega}_{v,k} = \arg\{\hat{z}_{v,k}\}$ from the roots' angles.
4) These frequencies correspond to the targets' range and relative velocity by the relations

$$\hat{d} = \frac{\hat{\Omega}_d c_0}{4\pi\Delta f} \text{ and } \hat{v} = \frac{\hat{\Omega}_v c_0}{4\pi f_c T_O}. \quad (14)$$

When allowing for values $P > 1$, this algorithm requires additional steps which may introduce further errors.

[2] Hence the algorithm's name, *Root MUSIC*, cf. [8], [10].

IV. Estimation Errors

A. Threshold effect

In [3] we show that the estimation is only reliable above a certain SNR threshold. We will term the region above this threshold the *high SNR range*. Of course, the estimation is not error-free even in this range. In order to gauge the error for distance and speed estimation, we make the assumption that the actual values for speed and distance are uniformly distributed within their respective unambiguous ranges.

The method we describe to estimate the precise threshold is computationally cumbersome and only works for the MLE case. For that reason, we will rely on simulations to determine the high SNR range.

B. Lower bounds

To calculate lower bounds for the estimation variance, we begin with the Cramér-Rao lower bound (CRB) for line spectra in one-dimensional processes. Its derivation is found in a multitude of publications (e.g. [7], [11]).

For a single complex sinusoid with unit amplitude in AWGN with noise power σ^2 and N discrete samples, the CRB for the estimate of the frequency assuming unknown phase is

$$\text{var}\{\hat{\omega}\} \geq \frac{6\sigma^2}{(N^2-1)N}. \quad (15)$$

To transfer this to the case of distance estimation, first assume we only have one OFDM symbol available. It consists of N values, and using (14), (15) can directly be converted into a CRB for the distance estimate:

$$\text{var}\{\hat{d}\} \geq \frac{6\sigma^2}{(N^2-1)N}\left(\frac{c_0}{4\pi\Delta f}\right)^2. \quad (16)$$

Calculating the CRB for the entire frame is highly complex due to the fact that the matrix $\mathbf{F}$ consists of M OFDM symbols, each with a different, random and unknown initial phase, due to the unknown Doppler shift. We make use of the fact that the presented estimators have some kind of implicit averaging to identify a simpler lower bound: We begin by stating that every OFDM symbol can be used for one estimation $d_i, i = 1 \ldots M$. As we have postulated *white* noise as the source of error, the d_i represent *independent* estimates of d. Probability theory tells us that by averaging, we obtain an estimate $\hat{d}$ with variance

$$\text{var}\{d\} = \frac{1}{M}\text{var}\{d_i\}. \quad (17)$$

We can apply this to (16), yielding

$$\mathrm{var}\{\hat{d}\} \geq \frac{6\sigma^2}{(N^2-1)NM}\left(\frac{c_0}{4\pi\Delta f}\right)^2. \tag{18}$$

We call this bound the *averaged* CRB because it is not a true CRB anymore, but is still a useful lower bound for the analyses presented here.

In a similar fashion, a lower bound for $\hat{v}$ can be given,

$$\mathrm{var}\{\hat{v}\} \geq \frac{6\sigma^2}{(M^2-1)MN}\left(\frac{c_0}{4\pi T_O f_c}\right)^2. \tag{19}$$

It is worth pointing out the influence of SNR on the bounds, since they both share dependencies. By using $\mathrm{SNR} = 1/\sigma^2$ and $B = N\Delta f$, we insert (8) into (18) and (19), yielding

$$\mathrm{var}\{\hat{d}\} \geq \frac{6(4\pi)N_0}{P_{\mathrm{Tx}}G} \cdot \frac{r^4}{\sigma_{\mathrm{RCS}}} \cdot \frac{f_c^2}{(N^2-1)M\Delta f}, \tag{20}$$

$$\mathrm{var}\{\hat{v}\} \geq \underbrace{\frac{6(4\pi)N_0}{P_{\mathrm{Tx}}G}}_{\text{Hardware}} \cdot \underbrace{\frac{r^4}{\sigma_{\mathrm{RCS}}}}_{\text{Target}} \cdot \underbrace{\frac{\Delta f}{(M^2-1)MT_O^2}}_{\text{Signal parameters}}. \tag{21}$$

Interpreting (20) and (21) gives three insights in particular into the system design:

- Given the point-scatter approximation, f_c only influences $\hat{d}$ in a manner that lowering the frequency decreases the lower bound.
- Increasing M decreases the lower bound for both estimates, but as this means increasing the signal duration, it also increases medium access and allows for less measurements per time unit[3].
- When increasing the bandwidth, it is advantageous to increase N rather than Δf. This is only possible within limits given by the channel characteristics, most importantly the channel's coherence bandwidth [4].

Finally, it must not be forgotten that the CRB is a suitable quality metric only for *unbiased* estimators, and comparing to the actual estimates only makes sense above the SNR threshold.

C. Quantization error

In case of the MUSIC-based algorithm, quantization becomes a negligible effect if we employ floating-point accuracy arithmetic.

For the MLE algorithm, this is different: Since the estimates $\hat{d}$ and $\hat{v}$ are strictly quantized, the estimation quality is affected by a quantization error. From the assumption that the true distances and velocities are uniformly distributed within their unambiguous ranges, the error variances caused by quantization are

$$\mathrm{var}\{\hat{d}\} \geq \frac{c_0^2}{12(2N_{\mathrm{FFT}}\Delta f)^2} \tag{22}$$

and

$$\mathrm{var}\{\hat{v}\} \geq \frac{c_0^2}{12(2f_c M_{\mathrm{FFT}} T_O)^2}, \tag{23}$$

[3]From a communication viewpoint, it reduces network capacity.

TABLE II
OFDM SIGNAL PARAMETERS

Δf	N	M	f_c	T_G
78.125 kHz	52	256	5.9 GHz	$1/4\Delta f$
90.9 kHz	1024	256	24 GHz	$1/8\Delta f$

respectively.

From (22) and (23), it is clear that increasing N_{FFT} and M_{FFT} improves the variance caused by quantization. This is achieved by zero-padding $\mathbf{F}$ before step 1) in the algorithm presented in Section III-A. The bias is also affected by this: For a fixed distance which does not exactly lie within the grid dictated by the system setup, the estimate *always* has a bias, which decreases when increasing the zero-padding. At the same time, the variance will decrease until it reaches the CRB, which leads to a maximum value of M_{FFT} and N_{FFT} beyond which increasing the zero-padding has no effect.

V. SIMULATIONS

We used simulations to empirically test the quality of the estimators. Two signal types were compared: A wideband OFDM signal in the 24 GHz ISM band, which we have mentioned in earlier publications (e.g. [3], [12]) and a signal parametrized very similarly to IEEE 802.11p signals [13], which are a common choice for car-to-car communications. These signals are very different in several aspects and so are good candidates to show the effects on the estimator statistics; the signal parameters are shown in Table II.

To be able to compare the results between the waveforms, we fixed all parameters except for the distance. The total noise figure was set to 20 dB, T was fixed at 290 K and the RCS to 10 m^2. For the simulation, the distance was increased from 10 m to 200 m in steps of 1 m. At every step, 1000 simulations were run at random velocities, uniformly distributed within ± 100 m/s.

The MLE was always set up with a four-fold zero-padding, i.e. $M_{\mathrm{FFT}} = 4M$ and $N_{\mathrm{FFT}} = 4N$.

Fig. 1 shows the average estimator distance bias at every step, as well as the variance for the distance and speed estimations. The speed bias was omitted, since v was chosen with a zero mean, which is the value an estimator will converge to when SNR is so low that all it can do is guess the estimate.

We can clearly see the threshold for each signal and estimator. For the threshold, the narrowband signal outperforms the wideband signal, and MLE outperforms the MUSIC estimator. The former is easily explained: With the given radio setup, the narrow-band signal has an SNR advantage since the noise power density is the same in both cases; also, it uses a lower centre frequency which yields lower path loss. This is also reflected in (18). SNR for every given distance is shown in Fig. 1b on a logarithmic scale to highlight the simple dependency on distance and bandwidth.

The latter effect is in fact a disadvantage of the MUSIC estimator; the estimation of the autocorrelation matrix requires a higher SNR than the MLE.

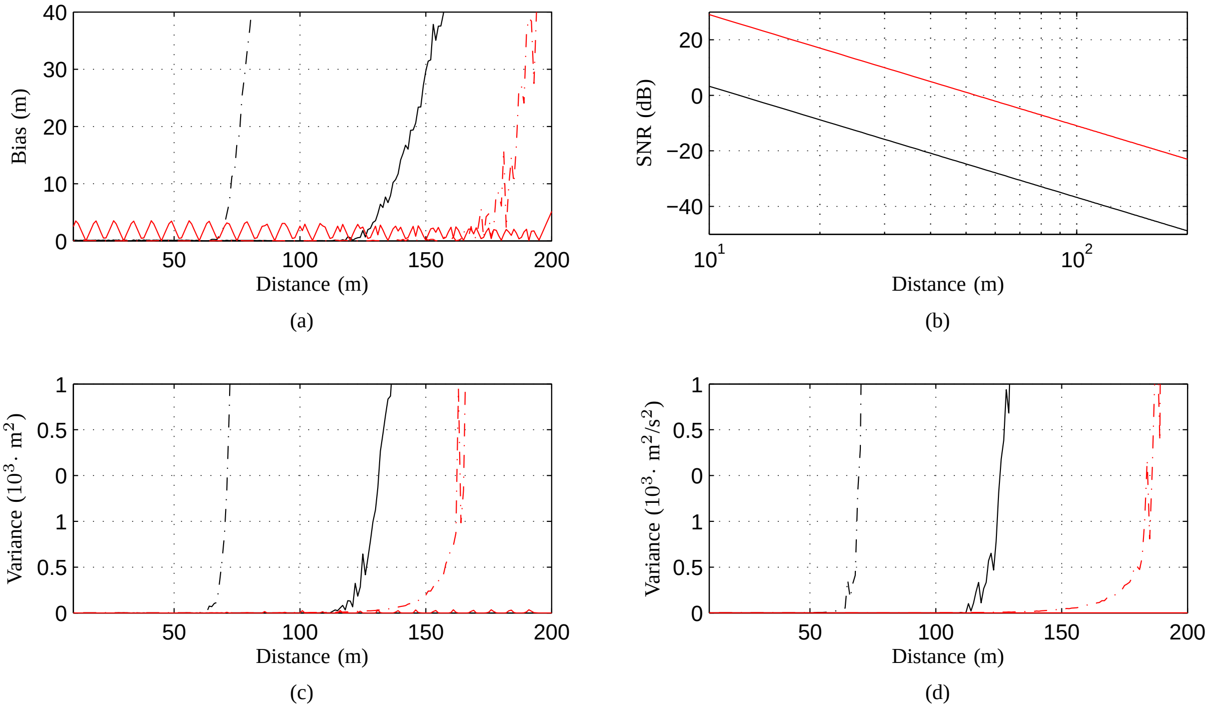

Fig. 1. The general performance of the MLE (solid lines) and MUSIC (dashed lines) estimators, for wideband (black lines) and narrowband signals (red lines). The top right image shows the SNR at the receiver at a given distance.

From Fig. 1a, we can see the quantization effect for the ML estimate on the narrowband signal: since the simulation runs along a different grid than the estimator, the bias increases and decreases periodically as it approaches and moves from the grid centres. This is not the case for the MUSIC estimates, as they have no quantization effect, and is not visible for the wideband signal which has a much finer grid.

Also notable is the fact that the MLE error for the narrowband signal is constantly close to zero. This must be interpreted with the right scrutiny: The quantization grid for this signal is fairly coarse, so as long as the threshold is not reached, the variance will naturally stay very low since the estimator will always choose the same bin. Besides, a lower bandwidth is a disadvantage when extending the case to more than one target.

VI. Conclusion

In this paper, we studied some fundamental limits of spectral estimation based OFDM radar algorithms. In particular, we identified some bounds for the estimator quality both analytically and empirically, in the case of a single target. While of course further research is required to extend these results to the case of multiple targets, simulations suggest that the OFDM radar approach is a very promising one. We believe that this kind of radar system can be added as an upgrade to systems which already use OFDM for a communications link, which might be useful for vehicular applications.

References

[1] C. Sturm, T. Zwick, and W. Wiesbeck, "An OFDM System Concept for Joint Radar and Communications Operations," *Vehicular Technology Conference, 2009. 69th IEEE*, April 2009.

[2] C. Sturm, M. Braun, T. Zwick, and W. Wiesbeck, "A Multiple Target Doppler Estimation Algorithm for OFDM based Intelligent Radar Systems," *7th European Radar Conference*, 2010.

[3] M. Braun, C. Sturm, and F. K. Jondral, "Maximum Likelihood Speed and Distance Estimation for OFDM Radar," *Radar Conference, IEEE International*, 2010.

[4] M. Braun, C. Sturm, A. Niethammer, and F. K. Jondral, "Parametrization of Joint OFDM-based Radar and Communication Systems for Vehicular Applications," *20th IEEE Symposium on Personal Indoor and Mobile Radio Communications*, 2009.

[5] T. Schipper, J. Fortuny-Guasch, D. Tarchi, L. Reichardt, and T. Zwick, "Rcs measurement results for automotive related objects at 23-27 ghz," in *Antennas and Propagation (EUCAP), Proceedings of the 5th European Conference on*, april 2011, pp. 683 –686.

[6] M. I. E. Skolnik, Ed., *Radar handbook*, 2nd ed. Norwich, NY: Knovel, 2003.

[7] D. Rife and R. Boorstyn, "Single tone parameter estimation from discrete-time observations," *Information Theory, IEEE Transactions on*, vol. 20, no. 5, pp. 591–598, Sep 1974.

[8] P. G. Stoica and R. L. Moses, *Introduction to spectral analysis*. Upper Saddle River, NJ: Prentice Hall, 1997.

[9] R. Schmidt, "Multiple Emitter Location and Signal Parameter Estimation," *Antennas and Propagation, IEEE Transactions on*, vol. 34, no. 3, pp. 276 – 280, Mar. 1986.

[10] A. Barabell, "Improving the resolution performance of eigenstructure-based direction-finding algorithms," in *Acoustics, Speech, and Signal Processing, IEEE International Conference on ICASSP '83.*, vol. 8, Apr. 1983, pp. 336 – 339.

[11] S. M. Kay, *Modern Spectral Estimation*. Prentice Hall, 1988.

[12] C. Sturm, E. Pancera, T. Zwick, and W. Wiesbeck, "A Novel Approach to OFDM Radar Processing," *Radar Conference, IEEE*, May 2009.

[13] *IEEE 802.11 Standard, Part 11*, 2005.